

An Interacting Multiple-Model-Based Abrupt Change Detector for Ground-Penetrating Radar

Vijayaraghavan Venkatasubramanian, Henry Leung, *Member, IEEE*, and Brian Moorman

Abstract—In this letter, we propose an interacting multiple-model (IMM)-based abrupt change detector for ground-penetrating radar (GPR) applications. Ground clutter varies with surface roughness, soil nature, as well as depth of the soil layer, necessitating a multiple-model approach. The IMM is first trained for a chosen number of models and then used to characterize the GPR data. The IMM predictor segments the entire GPR data into regions of identical models and then identifies targets by detecting abrupt changes in model parameters. The number of models is determined using the minimum prediction error criterion. The prediction performance of the IMM predictor is theoretically analyzed, and its detection performance is also evaluated through an receiver operating characteristics analysis to illustrate the improved performance of the proposed detector.

Index Terms—Change detection, clutter removal, ground penetrating radar (GPR), interacting multiple-model (IMM).

I. INTRODUCTION

GROUND-penetrating radar (GPR) is widely used for non-invasive investigation of subsurface object detection for its capability to detect even nonmetallic targets [1]. However, the performance of GPR is degraded due to the presence of clutter [2]–[4]. Ground clutter is, in general, nonstationary, and varies with depth and with soil inhomogeneities. The nonstationary nature of clutter introduces lot of false alarms in an energy detector [2].

It has been experimentally shown that a dominant interference in GPR data is correlated clutter [3]. Subsequently, parametric models have been proposed for ground clutter modeling, thereby resulting in several clutter reduction approaches, including likelihood ratio testing, principal and independent components analyses [4], recursive least squares (LS), and adaptive Kalman filtering [3]. The adaptive filtering approach first constructs a parametric model of GPR clutter [3] and uses a Kalman filter to estimate the parameter values at each time instant.

Parametric modeling of ground clutter overcomes some of the problems that are associated with the stationarity assumptions. However, the dielectric properties of the ground exhibits a spatial variation in both crosstrack (across scans) and down-

track [5]. Thus, a multiple-model (MM) approach was adopted for this study [6], in particular, the interacting MM (IMM) because of its lower complexity [6], [7].

In this letter, we propose a novel IMM-based abrupt change detector for GPR. In the proposed method, an IMM filter is used to predict the measured GPR data. The IMM predictor helps in the segmentation of measured GPR data into regions of identical models using probabilistic measures. These probabilistic measures are then used by the MM abrupt change detector to detect the presence of targets. The performance of the proposed detector is tested using GPR data from the PulseEKKO system [8] at the Yemen test site.

The rest of this letter is organized as follows. In Section II, we present the system formulation for MM GPR clutter modeling and preprocessing. In Section III, we present our proposed IMM-based abrupt change detector algorithm and the theoretical performance analysis of the IMM predictor. In Section IV, we present the results and performance analysis of the proposed detector for the measured GPR data sets. Finally, conclusions are drawn in Section V.

II. SYSTEM FORMULATION

The variations in the dielectric nature of soil with respect to depth cause a change in their reflection parameters. To illustrate this effect, an A-scan¹ is shown in Fig. 1. The changes are quantified by fitting an autoregressive moving average (ARMA) model to the GPR data. The variations in ground properties have an effect of introducing a change in the ARMA parameters of the return signal, as shown in Fig. 1. The order of the AR and MA portions were fixed at four each. The first four MA parameters of the ARMA model are plotted as a function of the sample number n . We observe that GPR A-scans follow MMs and can be modeled by different sets of regression coefficients. Each sample in a measured GPR A-scan is assumed to follow one of M finite number of models [7]. The n th sample point in a GPR A-scan that follows the m th model can be expressed as

$$z(n) = \theta_m^T \mathbf{x}_m(n) + w_m(n) \quad (1)$$

where θ_m is the parameter vector that corresponds to the m th model, $\mathbf{x}_m(n)$ is the state vector that contains delayed samples of the measured GPR A-scan $z(n)$ and that of the transmitted GPR excitation signal $u(n)$, and $w_m(n)$ is the measurement noise of the m th model, which is a realization of a white Gaussian random process with variance λ_m^2 . Further, the measurement noise $w_m(n)$ is assumed to

¹A-scan refers to GPR measurements that were taken at a particular point above the ground. B-scan refers to a collection of the collection of A-scans that were taken along a line above the ground.

Manuscript received September 14, 2005; revised August 2, 2006.

V. Venkatasubramanian is with SiRF Technology, San Jose, CA 95112 USA, and also with the Department of Electrical and Computer Engineering, University of Calgary, Calgary, AB T2N 1N4, Canada (e-mail: vijayv@sirf.com).

H. Leung is with the Department of Electrical and Computer Engineering, University of Calgary, Calgary, AB T2N 1N4, Canada (e-mail: leungh@ucalgary.ca).

B. Moorman is with the Department of Geography, Geology and Geophysics, University of Calgary, Calgary, AB T2N 1N4, Canada (e-mail: moorman@ucalgary.ca).

Digital Object Identifier 10.1109/LGRS.2007.896323

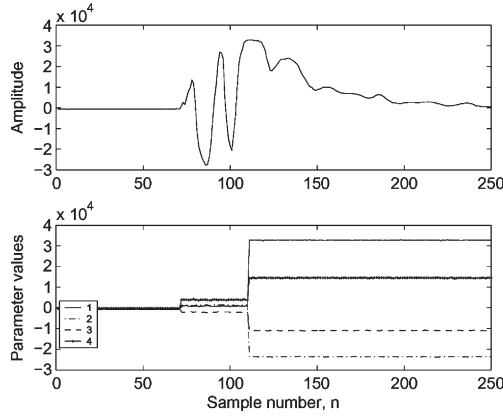


Fig. 1. Typical A-scan and variations in the model parameters.

be both spatially and temporally white. The GPR excitation signal $u(n)$ can be measured from the reflected waveform using reflection off a perfectly conducting material in a laboratory measurement. For an ARMA system assumption, the state $\mathbf{x}_m(n)$ is given by $\mathbf{x}_m(n) = [-z(n-1), \dots, -z(n-p_m), u(n), \dots, u(n-q_m)]^T$, and the parameter vector is given by

$$\boldsymbol{\theta}_m = [a_{m1}, a_{m2}, \dots, a_{mp_m}, b_{m0}, b_{m1}, \dots, b_{mq_m}]^T \quad (2)$$

where p_m and q_m are the orders of AR and MA filters of the m th model, respectively. The model order for MA and AR was also chosen through the minimum prediction error (MPE) criterion using the first A-scan from the data set, and the model orders were obtained as four for both AR and MA. An initial analysis of every tenth A-scan indicated very little change in model orders and parameters. In the present case, the GPR data set was collected over a length of 39.5 m, and soil properties were homogenous throughout the region. In larger data sets spanning a larger area, soil exhibits a huge variation in properties, and the learning algorithm is expected to use additional A-scans to train the model parameters.

Let $S(n)$ represent the model that is followed by the n th sample point of the GPR A-scan. $S(n) = m$ if $z(n)$ follows model m . Let $\mu_m(n)$ be the probability that the n th sample point in a GPR A-scan follows the m th model, given the prior information $Z^{n-1} = \{z(0), \dots, z(n-1)\}$. That is,

$$\mu_m(n) = P\{S(n) = m | Z^{n-1}\} \quad (3)$$

with the condition that $\sum_{m=1}^M \mu_m(n) = 1$ to quantify the fact that GPR samples follow either one of M possible models. The system undergoes Markov-process-based model switching with transition probabilities that are given by p_{ij} . p_{ij} denotes the probability that model j is followed at time instant n given that model i was in effect at $n-1$, and from the notations defined above, it can be written as $p_{ij} = P\{S(n) = j | S(n-1) = i\}$. In the case when the transition from state i to j and state j to i are equally likely, i.e., $p_{ij} = p_{ji}$, the model transition probability matrix is symmetric.

A single GPR A-scan is used to estimate the parameters of the different models. The optimal parameters of the m th model $\boldsymbol{\theta}_m$ are obtained by maximizing the likelihood function. In order to learn the different models, a Kalman smoother is used to perform segmentation. Under Gaussian noise with

a known segmentation, the maximum likelihood estimate of the parameter vector is equivalent to an LS estimate. We use the Steiglitz–McBride algorithm to obtain the LS estimates of the filter parameters in an iterative fashion. The LS estimate of the parameters that were obtained from the M segments are used as model parameters of M predictors in IMM. The model specific noise covariances λ_m^2 s are then obtained by estimating the variance of the prediction error covariance of each filter model $E(|w_m(n)|^2)$. In case of large data sets, the number of models and parameter sets is periodically updated to account for the variation of clutter statistics with distance.

III. IMM-BASED ABRUPT CHANGE DETECTOR

A. Algorithm

To predict a GPR A-scan, a set of M Kalman filters is run, and each is tuned to the M models of the clutter. Let $\hat{\mathbf{x}}_m(n)$ denote the estimated state vector of the m th model and $\mathbf{C}_m(n)$ denote its estimated variance. The input to the IMM predictor is the measured GPR signal $z(n)$. At each time instant, the initial conditions of the M Kalman filters are obtained from the previous state and covariance estimates through a step called interacting/mixing. The mixing probabilities are used to obtain the initial state and covariance estimates. Mixing probability, i.e., the probability that model l was followed at $n-1$, given that model m is followed at n , which is denoted by $\mu_{l|m}(n-1|n)$, is given by

$$\begin{aligned} \mu_{l|m}(n-1|n) &= P\{S(n-1) = l | S(n) = m, Z^{n-1}\} \\ &= \frac{1}{\alpha_m} p_{lm} \mu_l(n-1) \end{aligned} \quad (4)$$

where the normalizing constant $\alpha_m = \sum_{l=1}^M p_{lm} \mu_l(n-1)$. From the mixing probabilities, the mixed initial state estimates $\hat{\mathbf{x}}_m^-(n)$ and the covariance estimates $\mathbf{C}_m^-(n)$ for the m th Kalman filter can be expressed as a weighted sum of previous estimates, i.e.,

$$\begin{aligned} \hat{\mathbf{x}}_m^-(n) &= \sum_{l=1}^M \hat{\mathbf{x}}_l(n-1) \mu_{l|m}(n-1|n) \\ \mathbf{C}_m^-(n) &= \sum_{l=1}^M \left[\mathbf{C}_l(n-1) + [\hat{\mathbf{x}}_l(n-1) - \hat{\mathbf{x}}_m(n-1)] \right. \\ &\quad \left. \times [\hat{\mathbf{x}}_l(n-1) - \hat{\mathbf{x}}_m(n-1)]^T \right] \mu_{l|m}(n-1|n). \end{aligned} \quad (5)$$

The M Kalman filters are recursed to produce model conditioned state and covariance estimates, as well as the prediction of the GPR signal as

$$\begin{aligned} \hat{\mathbf{x}}_m(n) &= \hat{\mathbf{x}}_m^-(n) + \mathbf{K}_m(n) [z(n) - \boldsymbol{\theta}_m^T \hat{\mathbf{x}}_m^-(n-1)] \\ \mathbf{K}_m(n) &= \mathbf{C}_m^-(n) \boldsymbol{\theta}_m [\boldsymbol{\theta}_m^T \mathbf{C}_m^-(n) \boldsymbol{\theta}_m + \lambda_m^2]^{-1} \\ \mathbf{C}_m(n) &= [I - \mathbf{K}_m(n) \boldsymbol{\theta}_m^T] \mathbf{C}_m^-(n) \end{aligned} \quad (6)$$

where $\mathbf{K}_m(n)$ and $\mathbf{C}_m(n)$ are the Kalman gain and covariance estimate of the m th filter, respectively.

Finally, the model probabilities are calculated from the prediction error incurred in assuming a particular model. The predicted GPR A-scan of the m th Kalman filter at n th time

instant is $\hat{z}_m(n) = \theta_m^T \hat{\mathbf{x}}_m(n)$. The likelihood functions for each model on the prediction of $z(n)$, assuming a Gaussian error model, can be written as

$$\Lambda_m(n) = \frac{1}{\sqrt{2\pi\lambda_m^2}} \exp \left[-\frac{(z(n) - \hat{z}_m(n))^2}{2\lambda_m^2} \right]. \quad (7)$$

The model likelihood functions Λ_m , are used to assign the model probabilities $\mu_m(n)$. That is,

$$\mu_m(n) = \frac{1}{\alpha} \Lambda_m(n) \sum_{l=1}^M p_{lm} \mu_l(n-1) = \frac{1}{\alpha} \Lambda_m(n) \alpha_m \quad (8)$$

with $\alpha = \sum_{m=1}^M \Lambda_m(n) \alpha_m$.

The model probabilities of the IMM predictor can be used to detect the presence of targets using the abrupt change detector. Let us assume that $\mu_m^0(n)$ denotes the true model probabilities that were obtained from the training data of the n th sampling instant of a GPR A-scan. Here, we formulate a Kalman-filter-based abrupt change detector to detect and locate the targets. Under null hypotheses (i.e., absence of target), it is assumed that the model probabilities do not vary from those obtained from training data. Under this assumption, $\mu_m(n) = \mu_m^0(n)$. Whereas, in the presence of a target, there will be a large deviation of model probabilities from those obtained using training data set. The Kalman filter is run on this difference in model probabilities at each instant given by

$$\delta(n) = [\mu_1(n) - \mu_1^0(n), \mu_2(n) - \mu_2^0(n), \dots, \mu_M(n) - \mu_M^0(n)]^T \quad (9)$$

and the system model in the target-free case is

$$\delta(n) = \delta(n-1) + \mathbf{v}(n) \quad (10)$$

where $\mathbf{v}(n)$ is the error in the model probability estimates, which is assumed to be white Gaussian with a covariance matrix of Σ_v . The prediction error is given as $\epsilon(n) = \delta(n) - \hat{\delta}(n)$, where $\hat{\delta}(n)$ is the predicted state vector. A normalized version of the prediction error variance is used as the decision statistics to detect target.

B. Theoretical Analysis

The model probabilities are assigned based on the prediction error of the GPR signal. Hence, the prediction error performance is analyzed here. From the IMM filter (6), the final prediction of the n th sample of a GPR A-scan is given by

$$\hat{z}(n) = \sum_{m=1}^M \mu_m(n) \theta_m^T \hat{\mathbf{x}}_m^-(n) \quad (11)$$

where $\theta_m^T \hat{\mathbf{x}}_m^-(n)$ is the m th model conditioned prediction output of the n th sample of the GPR signal $\hat{z}_m(n)$. Therefore, (11) can be written as $\hat{z}(n) = \sum_{m=1}^M \mu_m(n) \hat{z}_m(n)$. The prediction error $\eta(n) = z(n) - \hat{z}(n)$ can be written as can be rewritten as

$$\eta(n) = \sum_{m=1}^M \mu_m(n) (z(n) - \hat{z}_m(n)) \quad (12)$$

since $\sum_{m=1}^M \mu_m(n) = 1$, the prediction MSE is then given by

$$E[|\eta(n)|^2] = E \left[\sum_{m=1}^M \sum_{l=1}^M \mu_l(n) \mu_m(n) \times (z(n) - \hat{z}_m(n)) (z(n) - \hat{z}_l(n)) \right] \quad (13)$$

where $E(\cdot)$ is the statistical expectation operation. Assume that the prediction errors of M predictors are zero mean and uncorrelated with each other, that is, $E[(z(n) - \hat{z}_m(n))(z(n) - \hat{z}_l(n))] = 0 \quad \forall m \neq l$. The MSE can be written as

$$E[|\eta(n)|^2] = \sum_{m=1}^M E \left\{ [\mu_m(n) (z(n) - \hat{z}_m(n))]^2 \right\}. \quad (14)$$

This equation indicates that the final prediction error of each filter λ_m^2 influences the final prediction error of the IMM predictor. Since the weighting factor for the previous model probability is assumed to be close to 0.9 in the steady state, the actual correlation between the model probability at a particular instant and error is only 0.1 when normalized with respect to the correlation between $\mu_m(n)$ and $\mu_m(n-1)$. Neglecting the cross correlation term, the prediction MSE can be approximated as

$$E[|\eta(n)|^2] \approx \sum_{m=1}^M E[\mu_m(n)^2] \lambda_m^2. \quad (15)$$

The GPR signal at any sample point n can be from either of the M models. Let p_m denote the ratio of time that a GPR A-scan follows model m to the total time of the GPR A-scan. The first term in (15) can be expressed as a sum of two independent terms as $E(\mu_m(n)^2) = p_m^2 + E[(\mu_m(n) - p_m)^2]$, where $E[(\mu_m(n) - p_m)^2]$ denotes the variance of the model probability function $\mu_m(n)$ and depends on the model transition probabilities. From the simulations, this term was found to be small, and hence, $E(\mu_m(n)^2)$ is approximated as the square of the average model probability p_m^2 . An approximated version of (15) can then be written as $E(\mu_m(n)^2) \approx \sum_{m=1}^M p_m^2 \lambda_m^2$. The approximated NMSE can then be obtained as

$$\text{NMSE} \approx 10 \log_{10} \frac{\sum_{m=1}^M p_m^2 \lambda_m^2}{\sum_{n=1}^N z(n)^2} \quad (16)$$

where N denotes the number of samples in a single GPR A-scan. The error introduced by the approximations is evaluated using data sets.

IV. RESULTS AND DISCUSSIONS

The proposed IMM-based abrupt change detector is applied to a measured real-life GPR data set to analyze its performance. The data set was obtained from walking tests conducted in Yemen using an ultrawideband GPR that operates at 100 MHz. The profile has 78 A-scans, spanning a distance of 39.5 m with

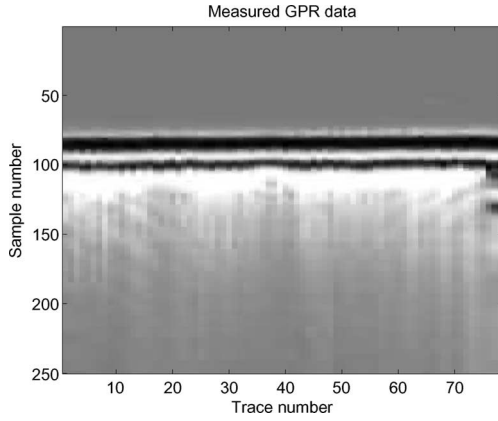


Fig. 2. Measured GPR data.

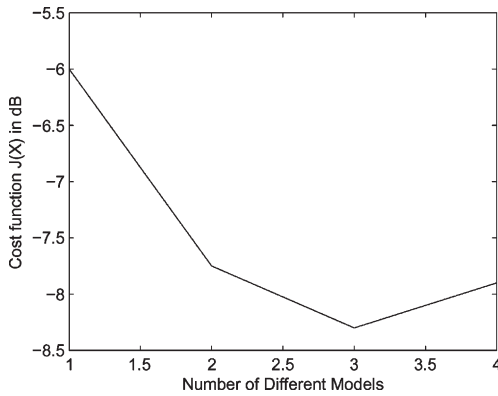


Fig. 3. MPE analysis.

0.5 m spacing between each A-scan. The targets here, if present, are usually boulders of various sizes. Each A-scan is an average of 128 consecutive returns sampled at 800 ps. A measured GPR image is shown in Fig. 2.

A. Model Number Selection

The choice of number of models M is a critical parameter while employing an IMM predictor. The MPE criterion is adopted here. Let X be the number of models with parameter vectors $\{\theta_m\}_{m=1}^X$. The prediction MSE defined as $1/N \sum_{n=1}^N \eta(n)^2$ implicitly depends on the number of models X and their parameters. The cost function is given by $J(X) = 1/N \sum_{n=1}^N \eta(n)^2$. The number of models M is found by obtaining X for which $J(X)$ is a minimum, i.e.,

$$M = \operatorname{argmin}_X J(X). \quad (17)$$

A plot of the prediction MSE for various numbers of models for the data set is shown in Fig. 3. The prediction error decreases with increasing number of models and reaches a minimum at $X = 3$. With the number of models fixed at three, we assume the transition probability matrix as

$$\begin{bmatrix} 0.9 & 0.05 & 0.05 \\ 0.05 & 0.9 & 0.05 \\ 0.05 & 0.05 & 0.9 \end{bmatrix}.$$

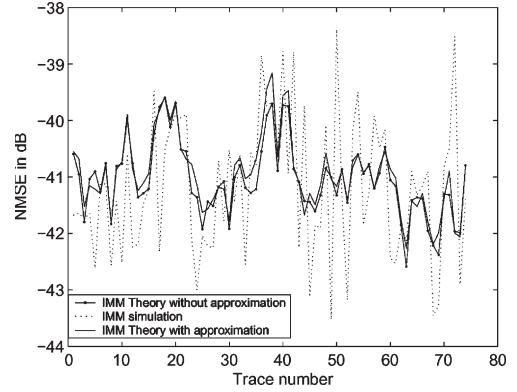


Fig. 4. IMM prediction performance.

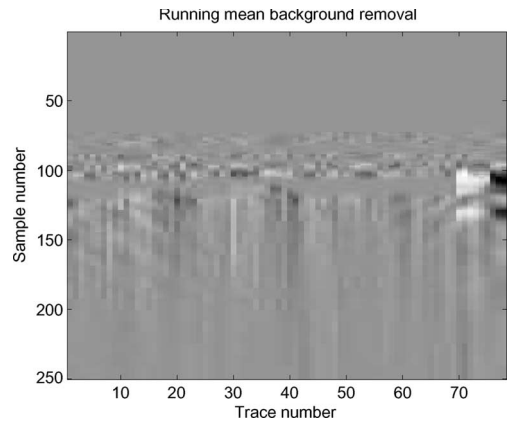


Fig. 5. Detected image using the mean removal technique.

B. Prediction Performance

To analyze the error performance of the IMM predictor, the NMSE measures are plotted in Fig. 4. It can be seen that the theoretical NMSE with and without approximation are close together, indicating that the approximation performed is valid. It can also be observed that the NMSE obtained through numerical simulations are close to the theoretical NMSE in most cases. A maximum prediction error of 3 dB for MSE figures of about -45 dB is observed in the data set corresponding to less than 7% approximation error.

C. Image Analysis

In the dataset, the target is known to be located in the last few A-scans of the B-scan data. For the data set, the clutter was removed using a background adaptation technique using a sliding window of size 10. The result is shown in Fig. 5. The gray scale is used here on the magnitude of the received signal response after mean removal. This technique eliminates most of the early time ground clutter. The distortions that are present in the image are due to the variations in ground clutter with distance and bias introduced in the background estimate due the presence of target. Kalman filtering was applied to the data in the data set. A small threshold that guarantees no false alarms is used here for both detectors. The resulting detected signal is plotted as a gray scale image and is shown in Fig. 6. The Kalman filter method is definitely better than mean removal

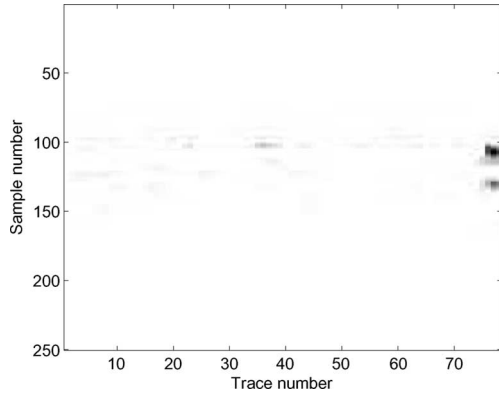


Fig. 6. Detected image using a Kalman filter.

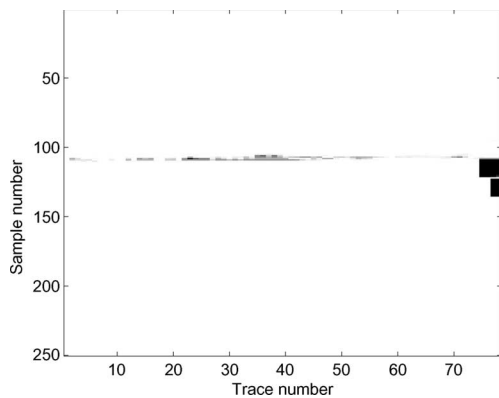


Fig. 7. Detected image using an IMM-based abrupt change detector.

technique. The background distortion is completely eradicated, avoiding false alarms. However, the target response is also suppressed, resulting in low contrast. The proposed IMM-based abrupt change detector with three models was run on the data set. The detected image is shown here in Fig. 7. The proposed detector results in an improved image contrast over both the Kalman filter and the mean removal techniques.

D. Receiver Operating Characteristic (ROC) Analysis

We compute the ROC performance using simulation analysis. A total number of 300 realizations of GPR A-scans were simulated from A-scans in the data set. A realization corresponds to randomly choosing one out of the 78 A-scans from the GPR data set. The standard detection methods, namely, Kalman detector and mean removal, followed by energy detector, were used for comparison. The ground truth data (four out of the 78 A-scans in the data set contained returns from the target) used in calculating the detection performance. The detection probability P_d is calculated by taking the ratio of the number of A-scans in which the presence of target was detected correctly to the total number of A-scans that contained a target. The false alarm probability P_{fa} is computed by taking the ratio of the number of A-scans that were falsely identified as targets to the total number of A-scans in which targets were not present. The number of A-scans with and without target were chosen to be equal. The ROC curves for the detectors are shown in Fig. 8. It can

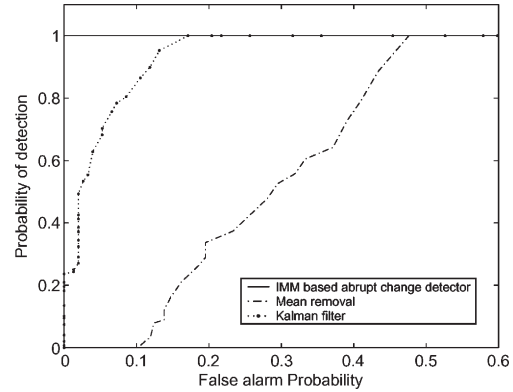


Fig. 8. ROC analysis of different detectors.

be noticed that the IMM-based method guarantees a higher probability of detection at the same given false alarm rate. The proposed IMM-based method achieves the same false alarm as the other techniques at significantly lower thresholds, thereby guaranteeing the detection of weaker targets that are left undetected by other conventional methods.

V. CONCLUSION

In this letter, we presented a novel IMM-based abrupt change detector for clutter reduction in GPR. The motivation comes from MM behavior of the GPR data. MMs are trained using a few clutter samples of the measured GPR data. The IMM predictor then segments the GPR data into regions of identical models using probabilistic measures such as model probabilities. The abrupt change detector uses the model probabilities of the IMM predictor to detect the presence of targets. It was shown using real data that the proposed IMM-based abrupt change detector consistently outperforms conventional clutter reduction techniques. A theoretical performance analysis of the proposed IMM predictor was derived to illustrate the performance improvement. An ROC analysis of the proposed technique also indicates a definite improvement in the detection performance over conventional techniques.

REFERENCES

- [1] L. Peters, D. J. Daniels, and J. D. Young, "Ground penetrating radar as a subsurface environmental sensing tool," *Proc. IEEE*, vol. 82, no. 12, pp. 1802–1820, Dec. 1994.
- [2] A. Merwe and I. J. Gupta, "A novel signal processing technique for clutter reduction in GPR measurements of small, shallow landmines," *IEEE Trans. Geosci. Remote Sens.*, vol. 38, no. 6, pp. 2627–2637, Nov. 2000.
- [3] L. Van Kempen, H. Sahli, J. Brooks, and J. Cornelis, "New results on clutter reduction and parameter estimation for landmine detection using GPR," in *Proc. GPR, 8th Int. Conf. Ground Penetrating Radar*, May 2000, pp. 872–879.
- [4] B. Karlsen, J. Larsen, H. B. D. Sorensen, and K. B. Jakobsen, "Comparison of PCS and ICA based clutter reduction in GPR systems for anti-personal landmine detection," in *Proc. 11th IEEE Signal Process. Workshop Stat. Signal Process.*, Aug. 2001, pp. 146–149.
- [5] J. Curtis, "Dielectric properties of soils," Joint Unexploded Ordnance Coordination Office, Sep. 1998. Tech. Rep.
- [6] Y. Bar Shalom, X. R. Li, and T. Kirubarajan, *Estimation With Applications to Tracking and Navigation*. Hoboken, NJ: Wiley, 2001.
- [7] F. Gustafsson, *Adaptive Filtering and Change Detection*. Hoboken, NJ: Wiley, 2000.
- [8] PULSE EKKO 100 Brochure, Jul. 2007. [Online]. Available: <http://geomonitoring.co.kr/pdf/pe100.pdf>